In-Parallel Passive Compliant Coupler for Robot Force Control

T A Dwarakanath, Carl D. Crane III, Joseph Duffy, Chad Tyler

Center for Intelligent Machines and Robotics
University of Florida
Gainesville, FL-32611, USA
352-392-0814, ccrane@ufl.edu

Abstract

This paper describes the design of a Passive Compliant Coupler for Force Control (PCCFC) based on an In-parallel mechanism. The optimal synthesis of the mechanism is performed with the objective of achieving a good quality index. The novel design of the connector (also termed as the leg), a crucial element of the mechanism, is one of the important features of the paper. The shape optimization of connectors of an in-parallel mechanism is obtained by satisfying compliant requirements and considering maximization of signal to noise ratio criteria. The various design aspects of sizing, sensing the displacement and implementation of the connector are discussed. The In-parallel compliant mechanism for force control is obtained by optimizing the signal to noise ratio at various stages of the mechanism design.

1.0 Introduction

The geometrical form of the in-parallel mechanism is quite complementary to that of the serial manipulator and so are its functional properties. The in-parallel mechanism is therefore perceived to be a good counterpart of a serial manipulator to complement the functional requirements of the task. The parallel mechanism has high load bearing capacity because its connectors sustain the payload in a distributive manner as long as it is far from a singular configuration. The error generated at each connector is not cumulative unlike the serial connected linkages in a serial mechanism. The in-parallel mechanism also aids in designing compact systems. High load bearing capacity, high positional accuracy, and the possibility of designing compact systems allows the parallel mechanism to be applied to a wide variety of applications. One such application is force control of serial manipulators where the parallel mechanism is mounted at the end of the serial arm and senses all the components of force encountered by the serial robot. This paper describes the design and development of a small compliant force-torque sensor based on an in-parallel mechanism.

The compliant parallel mechanism is to regulate force and displacement simultaneously by mapping a small infinitesimal twist between the two rigid bodies into the corresponding wrench that acts between them [Griffis and Duffy, 1991]. In active compliance control, the compliance of the connectors is adjusted by servos to obtain a linear relation between the force and displacement [Sugar and Kumar 1998]. The other approach is to control forces by controlling positions or controlling positions and forces together, such as compliant control, compliance and force control, and hybrid control. The above control methods are more difficult and require sophisticated instruments to build the controllers.

On the other hand passive compliance motion control can accommodate the misalignments that exist between two mating parts due to geometrical uncertainties and manufacturing tolerance of the parts. Passive compliance would be sufficient to sustain the required contact force between two interacting surfaces and most importantly would assist in the smooth transition of forces from the no contact mode region to contact with the environment. The simple and real-time response of passive control avoids the complex controller and sophisticated instrumentation required in some industrial applications. The in-parallel mechanism offers a straightforward and easy method to reconstruct the wrench applied on one of the plates from measured connector forces, therefore the Passive Compliant Coupler for Force Control (PCCFC) can provide force feedback control of the robot. It is different from commercially available Remote Center Compliance (RCC) devices which are open loop systems and not meant to sense the applied wrench and hence cannot provide force feedback control of the robot.

Gaillet and Reboulet [1983] developed the first sensor of this kind based on the octahedral structure of the Stewart platform. Nguyen et al [1991] reported the development of a Stewart platform based sensor with LVDT's mounted along the legs for wrench measurement in the presence of a passive compliance. Bhaumick et al [1997] reported the development of stiff force-torque sensor based on the Stewart Platform with shape optimization of the legs to minimize the signal to noise ratio. Various authors carried out theoretical investigations of the behavior of the Stewart platform sensor. Svinin and Uchiyama [1995] have considered the optimality of the condition number of the force transformation matrix. The optimum condition number criterion has to be exercised with utmost care. Though the optimum configuration appears

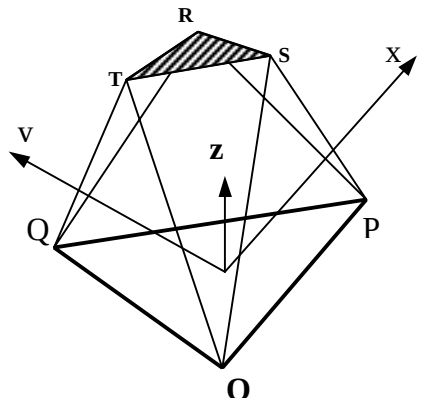

Figure 1: 3-3 In-Parallel Mechanism

to present an isotropic solution, the neighborhood solutions (configurations) may deteriorate very fast and could be close to a singularity. Therefore the condition number criteria can be at best limited to stiff Stewart Platform Sensors [Dasgupta, et al 1994, Bhaumick et al 1997] where a change in structural configurations is not anticipated and the condition number remains the same. Lee et al [1996] defined the problem of 'closeness' to a singularity measure by defining what is known as Quality Index (QI) for planer in-parallel devices. Lee et al [1998] extended the definition of Quality Index to spatial 3-3 in-parallel devices. The quality index is the ratio of the absolute value of the determinant of the Jacobean of the platform in some arbitrary position to the maximum absolute value of the determinant that is possible for the same in-parallel mechanism. However there is no proper mathematical basis to compare the performance of the two in-parallel systems as yet. The practical implementation of the parallel device based on theoretical studies present numerous problems. Hunt and McAree [1998] present an in-depth implication of such constraints and realistic design ideas.

2.0 Kinematic Model and PCCFC Specifications

The six-degree of freedom in-parallel mechanism has six connectors and they are connected through concentric spherical joint balls in a pair wise manner at the top and at the base. The top and bottom surfaces are considered to be planar for the sake of simplicity. The in-parallel mechanism in its best form should be fully triangulated to form a 3-3 octahedron. A schematic sketch of the in-parallel mechanism is given in Figure 1. This simple kinematic structure is complex to design. One, because of the problem of designing concentric joint balls and the other is due to the mechanical interference of closely arranged legs. To overcome the interference of legs, various ways of locating a leg along intended line coordinates is studied. Each of the six legs is a serial SPS (spherical-prismatic-spherical) chain.

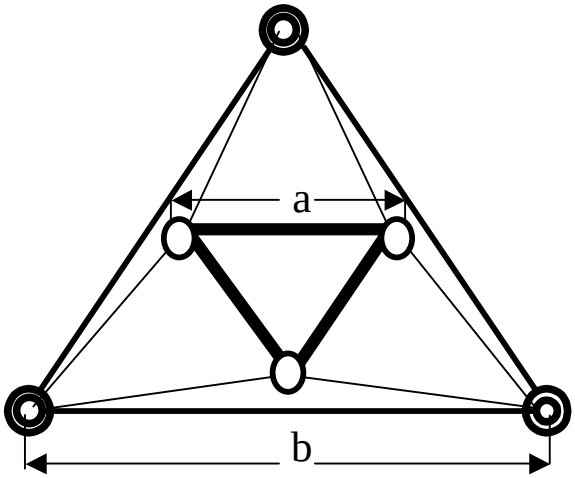

Figure 2: Top View of 3-3 Parallel Mechanism

The kinematic structure and the relative dimensions of the in-parallel mechanism are obtained by applying the optimal Quality Index criteria [Lee, et. al, 1998]. The Quality index (QI) is defined by following dimensionless expression.

$$\lambda = \frac{|\text{DetJ}|}{|\text{DetJ}|_m} \tag{1}$$

where DetJ is the determinant of the Jacobian which is a 6×6 matrix formed by the line co-ordinates of the 6 legs. The normalized determinant of the Jacobian, DetJ, at the central position and when both base and platform are parallel (as shown in Figure 2) is given by

$$|\text{DetJ}| = \frac{3\sqrt{3}a^3b^3h^3}{4\left(\frac{a^2-ab+b^2}{3}+h^2\right)^3} \tag{2}$$

where a and b are the sides of the equilateral triangle of the platform and the base respectively, h is the height of the platform measured from center of the base plate to the center of platform along z axis (see Figure 2). The above expression is optimized to find the expression for maximum |DetJ|. The maximum QI occurs when either of the following two parametric relationships is satisfied.

$$b = 2a \;;\; h = a$$

or (3)

$$a = 2b \;;\; h = b\,.$$

For a static force analysis, an external wrench $\vec{W}_0$ =[F_x, F_y, F_z, M_x, M_y, M_z] is applied to the movable platform. The relationship between the external wrench and the six leg forces is given by

$$\vec{W}_0 = \sum_{i=1}^{6} f_i \hat{s}_i \qquad (4)$$

where, f_i, i=1..6, are the magnitudes of the axial reaction forces experienced by the legs and $\hat{s}_i$, i=1..6, are the line co-ordinates of the legs. The system of forces remains in static equilibrium as the moveable platform twists relative to ground. To account for the twist, the external wrench changes as the platform moves. The mapping of the change in wrench to the twist of the platform is given by

$$\hat{W} = [K]\hat{D} \qquad (5)$$

where $\vec{W} = [\partial\vec{f}; \partial\vec{m}_0]$ is the change in wrench, which is mapped via 6×6 stiffness matrix [K] to the twist of the movable platform relative to the ground. The six twist co-ordinates give the twist $\hat{D} = [\partial\vec{x}_0; \partial\vec{\phi}_0]$. The expression for the global stiffness is given by Griffis and Duffy [1991] as

$$\begin{aligned}[K] = {} & [j][k_i][j]^T + [\partial j_\theta][k_i(1-\rho)[\partial j_\theta]^T \\ & + [\partial j_\alpha][k_i(1-\rho)[\partial j_\alpha]^T + [\partial j_\theta][k_i(1-\rho)[v_\theta]^T \\ & + [\partial j_\theta][k_i(1-\rho)[v_\alpha]^T \end{aligned} \qquad (6)$$

where the columns of the 6×6 matrices [j], [δj_θ] and [δj_α] are line coordinates. The i^{th} column of [j] is the line co-ordinate for the line $\$_i$ for the i^{th} leg, the i^{th} column of [δj_θ] is the line coordinate of the derivative $\delta\$_i^\theta$ with respect to the appropriate θ. θ_i defines the elevation angle of the plane of the triangle, which is formed by the end points of the i^{th} connector with the adjacent connector that shares the base edge, from the XY plane. ρ_i is the ratio of free length to the new length of the i^{th} leg (l_{0i}/l_i). The i^{th} column of [δj_α] is the line coordinate of the derivative $\delta\$_i^\alpha$ with respect to the appropriate α_i. The term α_i defines the oriented angle of the i^{th} connector measured from the base edge. [v_θ] and [v_α] are 6×6 matrix moment vectors and are explained in Griffis and Duffy [1991].

The objective of this paper is to design a small passive compliant coupler based on an in-parallel mechanism for force control. The desired load supporting ranges and compliance characteristics are given in Table 1. The values shown in the table are with respect to a right-handed co-ordinate system (xyz) defined at the center of the bottom plate (see Figure 1).

The following section deals with the mechanical design of a leg so as to achieve the desired compliance and payload characteristics.

Table 1: Desired Load and Compliance Characteristics

Sensing Axis	Ranges	Compliance	Resolution
Fx	± 25 N	± 4 mm	0.25 N
Fy	± 25 N	± 4 mm	0.25 N
Fz	± 60 N	± 8 mm	0.25 N
Mx	± 500 N-mm	18°	2.5 N-mm
My	± 500 N-mm	18°	2.5 N-mm
Mz	± 1000 N-mm	18°	2.5 N-mm

3.0 Mechanical Design of the Connector

The stiffness matrix of an in-parallel mechanism depends upon the kinematic arrangement of the legs as well as on the individual stiffnesses of the legs. The crucial design element as far as instrumentation is concerned is the connector, a part that connects the base plate and the top plate. The form of the connector has no kinematic consequence and hence the Quality Index is independent of the geometric form of the connector. Therefore choice of the form of the connector is made to enhance the performance of the sensor in terms of sensitivity, accuracy, repeatability, and ease with which it can be manufactured.

3.1 Form of the leg

The deflection of a leg is used as the measure of an applied force. Low stiffness of a leg would result in higher compliance, thus high force sensitivity. However the stiffness of the leg is guided by the specified minimum stiffness of the robotic arm since the sensor is generally connected to the end of the manipulator serially. The advantage of using an in-parallel passive mechanism as a force-torque sensor is that the leg stiffness can be much lower compared to the stiffness of the robotic arm because of its parallel arrangement. Therefore the parallel architecture for a compliant force-torque sensor at the end of a serial manipulator is a good choice.

The legs, acting as elastic elements, must be carefully designed so as to give proper resisting and restoring characteristics when the dynamic force is applied. Various geometrical forms of the leg were considered for the design. A sensor with tubular elements as the legs requires very small cross-sectional area to withstand the stress. However to account for buckling effect, an increase in cross-sectional area must be considered. This would increase the stiffness of the leg and thus seriously affect the overall sensitivity of the sensor. Ring shaped legs seem to be more promising and closely fit the requirement of the application. The design of

the ring shaped elastic elements is carried out by using the bending moment equation for thin rings (radial thickness of the ring is small compared to the radius of the ring). The ratio of deflection of the ring element due to the bending moment to that of the normal force represents the S/N ratio and hence is used as the objective function to design the cross-section of the ring element. The design analysis of the leg is made by considering a circular ring under the actions of two equal and opposite forces acting along a vertical diameter. Due to symmetry only one quadrant of the ring need to be considered. The bending moment, M of the ring at any cross section, defined by angle ϕ may be calculated by the following expression given by Timoshenko [1955],

$$M = \frac{f\,R}{2}(\cos\phi - \frac{2}{\pi}) \tag{7}$$

where f is the leg force experienced by ring element along its diameter. R is the radius of centroidal axis of the ring. The maximum bending moment can be obtained by substituting, $\phi=\pi/2$ in the above equation. The Maximum bending moment is given as

$$M = -0.318\,f\,R\,. \tag{8}$$

The increase in diameter of the ring or in other words the deflection of the leg is given by

$$\partial l = 0.149\frac{f\,R^3}{E\,I} \tag{9}$$

The compliance of the leg, $\delta l/f$, depends on the radius and cross-sectional dimensions of the ring for a chosen material. The ring dimensions are subjected to the constraints that (1) the bending stress due to the maximum force should be well within the elastic limit, (2) the radius of the ring should satisfy the dimensional constraints of the platform. The cross-sectional dimensions of the ring should be checked against failing due to buckling effects.

The desired ranges of force (as given in Table 1) along different axes are used to find the maximum axial force, f_{max}, applied to a single leg. The desired compliance of the in-parallel platform is used to find the maximum compliance required at each leg. It is found that the single ring element subjected to the design constraints as mentioned above cannot sustain the axial leg force while satisfying the desired compliance. In order to have a desired compliant system and yet support the specified force, a serial arrangement of the ring elements is designed. Such an arrangement not only results in higher compliance but also allows higher axial force. The arrangement is shown in figure 3a.

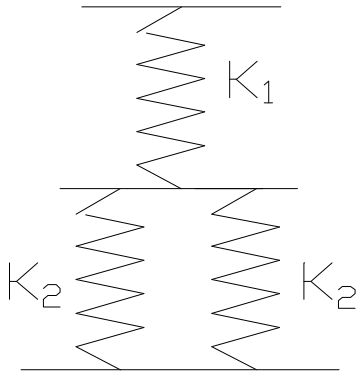

Figure 3a: Elastic Elements of the Leg

The required stiffness of the leg K_e, is modeled as follows:

$$K_1 = \frac{2f_{max}}{x} \tag{10}$$

where, K_1 is the stiffness of the one of the rings connected in series. The second ring in series is modeled as a parallel arrangement of two rings to avoid buckling, which also optimizes the overall size of the leg. The stiffness of one of the ring elements in parallel is given as

$$K_2 = \frac{f_{max}/2}{x/2} \tag{11}$$

The equivalent stiffness of the leg K_e is given by

$$K_e = \frac{2K_2K_1}{2K_2 + K_1} \tag{12}$$

which can be written as

$$K_e = \frac{f_{max}}{x} \tag{13}$$

where x is the required maximum deflection of the leg. The serial and parallel arrangement of the ring should be done very carefully to satisfy the size constraints of the leg. Figure 3b shows the optimized compact arrangement of the rings.

Further enhancement of the S/N ratio can be considered by compressing the circular ring to an elliptical form. Figure 4 shows the variation of stress at a critical section with respect to distance from the center to the critical section. It can be seen that for the same sensitivity of the leg,

Figure 3b: Compact Arrangement of Elastic Elements

the required major axis of an elliptical element is less than the diameter of a ring element.

Also, the height of the platform, which is the important optimizing parameter, can be shrunk by a factor of R_{maj} $(C_m-1)/C_m$, where C_m is the compression factor R_{maj}/R_{min}. The minimum leg length in the case of the ring element should be greater than the diameter of the ring, which poses difficulties in conforming to optimal sizing. In the case of the elliptical form the minor diameter of the ellipse lies along the length of the leg thus resulting in a more compact design.

3.2 Operating requirements

A prototype of the connector has been manufactured based on the above design and subjected to various tests to establish the static and dynamic behavior of the leg. The connector, an elastic element of the PCCFC system has been tested for linearity. Several static load tests were conducted to measure the deflection and all the results show satisfactory linear behavior of the elastic element. A slider crank mechanism is used to convert linear deflection into rotary motion. The mechanism is designed such that the transmitting angle is always in the neighborhood of the optimum transmission angle for the best transmission efficiency. A potentiometer is used to measure the rotary displacement. Figure 5 shows the force versus deflection from one of the sets of test data. The test data has resulted in good regression constant of 0.9967 for a straight-line fit.

The operating frequency of the serial robot for various assembly tasks is less than 100 to 150 rpm. The connector is subjected to dynamic testing to ascertain its response at various operating frequencies. Figure 6 shows the response of the connecter when subjected to a dynamic load varying at 6 Hertz.

3.2 Instrumentation and Interface

The deflection of the leg can be sensed by various techniques. A strain gauge can be bonded at the section of highest bending moment. Strain gauges could not be used in this case because the expected strain levels due to large displacement across the spring elements is very high (30%) and none of the commercially available strain gauges can measure such high strains. The other straightforward technique is to use a LVDT as a displacement-sensing device. This was not done because of the larger size and the higher cost compared to other alternatives. The deflection of the leg is sensed by a mini potentiometer connected across the spring elements of the leg. A slider crank mechanism is used to convert the axial deflection of the spring to angular deflection, which is sensed by a single turn, 5kΩ precision potentiometer driven by 5 Volts. A 12 bit, 40 kHz A/D converter is used to convert potentiometer data into digital form. Figure 7 shows the instrumentation arrangement of the connector.

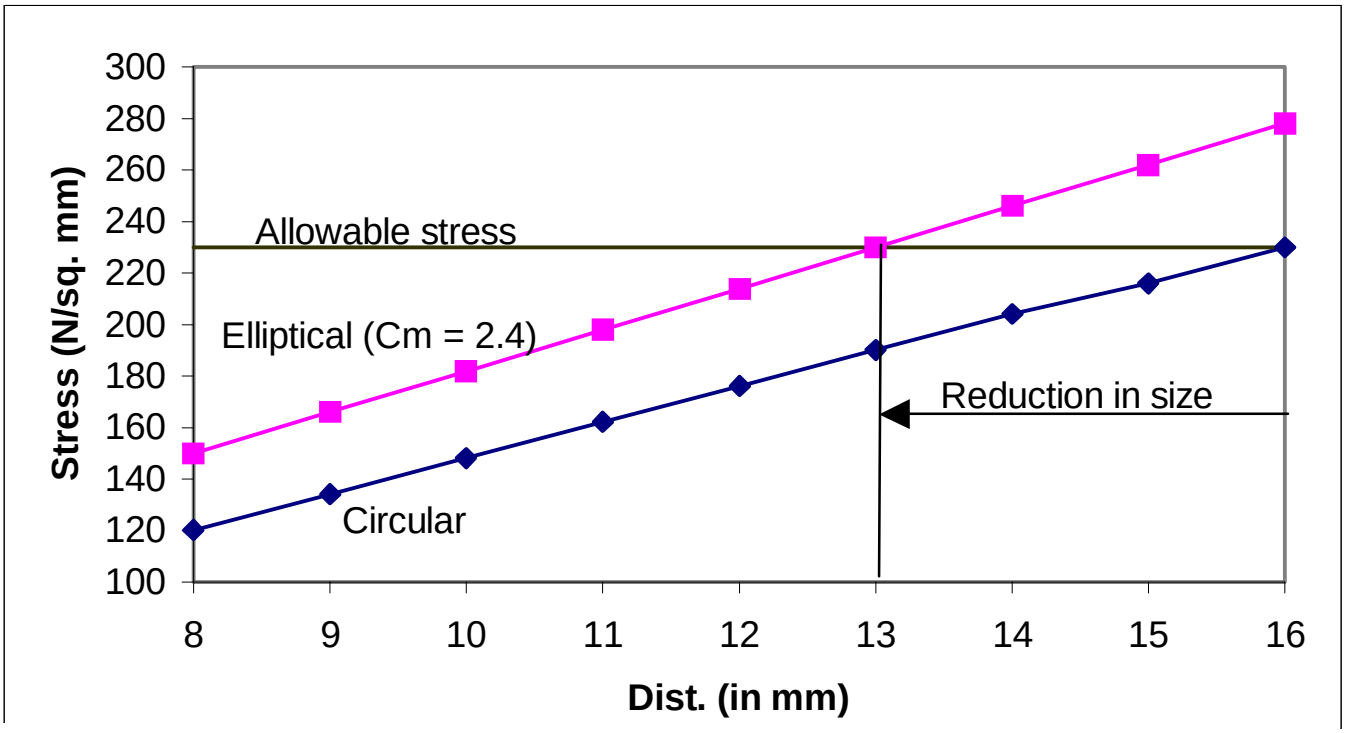

Figure 4: Stress at the Critical Section at Different Radii and Major Axes Distances

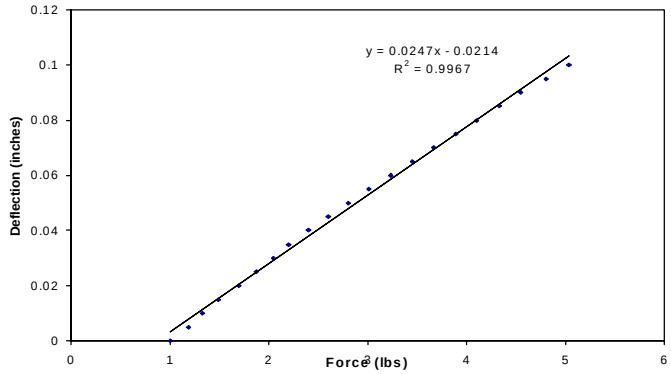

Figure 5: Static Load Test Depicting the Linearity of the Connector

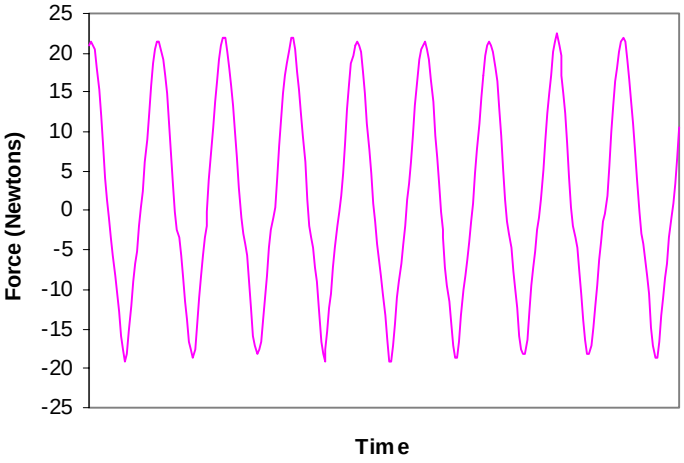

Figure 6: Dynamic Load Test at 6 Hertz Depicting the Response of the Connector

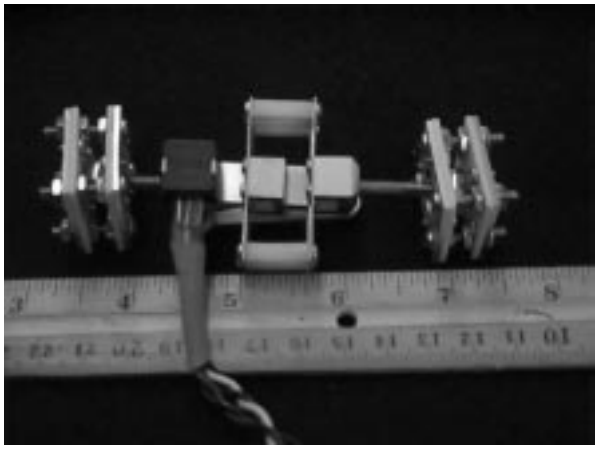

Figure 7: Instrumentation of the Connector

The maximum angular deflection range is a fractional part of the potentiometer's range. An appropriate voltage is applied across the potentiometer to match the sensor's output voltage to the A/D converter's input range. The angular position information from each displacement sensor is fed through separate A/D channels. The digital data is then made available to a personal computer through a parallel I/O port. The PC can compute the applied wrench after receiving data from all the six channels.

4.0 System Compliance

The leg design presented in section 3 is utilized to design a small compliant in-parallel mechanism based force-torque sensor. Figure 8 shows a model of an in-parallel compliant sensor with one possible way of arranging the legs. The central position of the platform is designed for a maximum Quality Index, which ensures that the in-parallel mechanism is farthest from a singular position. Based on the maximum Quality Index criteria the following values for the kinematic design parameters are obtained, which satisfy the desired specifications given in Table 1.

Base radius, (R_b) = 50.0 mm

Platform radius (R_p) = 25.0 mm

Side of base triangle, $S_b = 2.0\ R_b \cos\frac{\pi}{2}$

Side of platform triangle, $S_p = S_b/2$

Height of the platform, $h = S_b/2$

Free length of the leg, l_{0i} = 61.237 mm

Based on the leg design:

Number of spring elements in series, $N_s = 2$

Radius of the ring element, R_{ca} = 20 mm

Radial thickness of the ring element, d_{ca} = 0.45 mm

Width of the ring element, w_{ca} = 5 mm

The kinematics and structural dimension satisfies all the desired specifications except that the load it can support along the x and y axes are smaller than the desired specifications. The global stiffness matrix for the above described platform at its home position is given below.

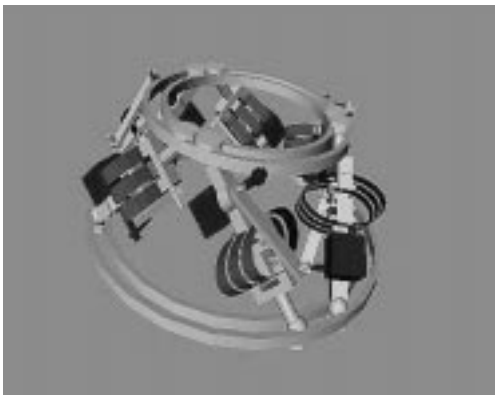

Figure 8: Model of In-Parallel Sensor

.

$$[K]=\begin{bmatrix} 10.9 & 0 & 0.63 & 7.9 & 444.5 & -272.2 \\ 0 & 10.9 & 0 & -472.3 & 7.9 & 472.3 \\ 0.63 & 0 & 21.91 & 547.7 & -921.7 & -15.8 \\ 7.9 & -477.1 & 547.7 & 41202 & -23033 & -21254 \\ 449.3 & 7.9 & -976.5 & -24403 & 68589 & -10901 \\ -272.2 & 527.2 & -15.8 & -23421 & -10762 & 43329 \end{bmatrix}$$

where the 3×3 sub-matrix have the following units:

upper-left: N/mm upper-right: N

lower-left: N lower-right: N-mm.

The natural frequency of the individual ring elements is very high compared to the operating frequency of the sensor, the frequency and the phase response of the system is expected to be good. For the compliance obtained, the dynamic amplitude response of the leg is also expected to be satisfactory.

5.0 Conclusion

A design of a small compliant in-parallel force-torque sensor is presented. The S/N ratio of the system is optimized at various design stages to enhance the sensitivity as well as the accuracy of the system. The compact design is made possible by optimizing the form of the connector. The central position of the platform is designed for maximum Quality Index, which ensures that the in-parallel mechanism is farthest from a singular position. The compliant sensor when connected to the end of the serial robot can be very helpful in carrying out many assembly tasks in force feedback mode. The assumption that connecting points lie on a planar surface is one of the factors that resulted in a sensor with preferential direction in supporting loads. Such preferential direction is advantageous in many robotic applications. The design of an isotropic sensor is still an open problem.

Acknowledgement

The first author greatly acknowledge the support of Department of Science and Technology, Government of India for providing Fellowship and Travel grants and Center for Intelligent Machines and Robotics for extending the facility to carry out this work. The Department of Energy is also gratefully acknowledged for its support via the University Research Program in Robotics, Grant No. DE-FG04-86NE37967.

References

Bhaumick T K, Dwarakanath, T. A, Venkatesh, D., 1997, ``Instrumentation of Stewart platform based force-torque sensor'', Proc. of symposium on Allied Nuclear Advances in Instrumentation , Bhabha Atomic Research Center, Mumbai, India, pp. 309-315.

Dasgupta B., Reddy S , Mruthyunjaya T S., 1994, ``Synthesis of a force-torque sensor based on the Stewart platform mechanism'', Proc. National Convention of Industrial problems in Machines and Mechanisms (IPROMM'94), Bangalore, India, pp. 14-23.

Griffis, M. and Duffy, J., 1991, ``Kinestatic Control: A Novel Theory for Simultaneously Regulating Force and Displacement'', Trans. ASME, Journal of Mechanical Design, vol. 113, pp. 508-515.

Gaillet, A and Reboulet, C., 1983, ``An Isostatic Six Component Force and Torque Sensor'', Proc. 13th Int. Symposium on Industrial Robotics.

Hunt, K. H., and McAree, P. R., 1998, ``The octahedral manipulator: geometry and mobility. International Journal of Robotic Research, Vol. 17, no. 8, pp. 868-885

Kerr, D. R., 1989 ``Analysis, Properties and Design of Stewart Platform Transducer'', Trans. ASME Journal Mechanical Transmission Automation and Design. Vol. 111, pp. 25-28.

Lee, J., Duffy, J., and Keler, M. 1996, ``The optimum quality index for the stability of in-parallel planar platform devices'', Proc. of ASME design engineering technical conferences, published on CDROM, 96-DETC/MECH-1135, Irvine, California, USA.

Lee, J., Duffy, J., and Hunt, K. H, 1998, ``A Practical quality index based on the octahedral manipulator'', International Journal of Robotic Research, Vol. 17, no. 10, pp. 1081-1090

Nguyen, C.C., Antrazi,S.S., and Zhou,Z.L., 1991, ``Analysis and Implementation of a 6 DOF Stewart Platform-Based Force Sensor for Passive Compliant Robotic Assembly'', Proc. IEEE SOUTHEASTCON, pp. 880-884.

Stewart, D., 1965, ``A Platform with Six Degrees of Freedom'', Proc. Inst. Mech. Engrs. Part I 180(15), pp. 371-386.

Sugar, T. and Kumar,V., 1998, ``Design and Control of a Compliant Parallel Manipulator for a Mobile Platform'', published on CDROM, 98-DETC/MECH-5863, Atlanta, Georgia, USA.

Svinin, M.M., and Uchiyama, M., 1995, ``Optimal Geometric Structures of Force/Torque Sensors'', International Journal of Robotics Research, vol. 14, no. 6, pp. 560-573.

Timoshenko S, Strength of Materials. Part II, 2nd ed. New York: D. Van Nostrand, Inc., 1955